Mathematical Model and Stability Analysis for Dusty-hybrid Nanofluid over a Curved Surface with Cattaneo–Christov Heat Flux and Fourier law with Slip Effect

Zeeshan[1], Waris Khan[2,*], Mariam Redn Almutiri[3], Badria Almaz Ali Yousif[4], Abeer A. Shaaban[5,6]

[1]Department of Mathematics and Statistics Bacha Khan University Charsadda, KP, Pakistan.
[2]Department of Mathematics and Statistics, Hazara University Mansehra 21120, Khyber Pakhtunkhwa, Pakistan
[3]Department of Mathematics, College of Science and Arts, Qassim University, Dariyah 58214, Saudi Arabia

[4]Department of Mathematics, College of Science and Arts, Qassim University, Unayzah 51911, Saudi Arabia

[5]Department of Mathematics, Faculty of Education, Ain Shams University, Heliopolis, Cairo, Egypt

[6]Department of Management Information Systems, College of Business Management, Qassim University, Ar Rass, Saudi Arabia

*Corresponding: dr.wariskhan@hu.edu.pk, wariskhan758@yahoo.com (Tel: +923028397271)

Abstract: The current study scrutinizes the influence of heat energy and slip effect using hybrid nanofluid suspended in the Ethylene–Glycol as a based liquid over the curved surface impinging Modified Fourier Law surrounding dust nanoparticles. The modeled mathematical equations in term of partial differential equations are transformed to convectional differential equations and are computed numerically via Finite Element Method. The flow characteristics are examined by assign numerical values to the physical parameters. The novelty of the problem is to examine the stability of dusty-hybrid nanofluid with slip effect. The hybrid nanofluid effectiveness is significantly higher compared to that exhibited by the traditional nanofluid. The consequences of the first-order slip variable, the curved variable, and the pulling force contribution on the velocity field, dust phase velocity, temperature field and dust phase temperature all increase with time. For different magnitudes of nanoparticles solid volume fraction, opposite behavior is observed for velocity field and dust phase velocity. The heat of the fluid drops in relation to the thermal relaxation coefficient. For the endorsement of the mathematical flow system error approximations has been computed. For the stability analysis a comparison of the current work is done with the published work.

Keywords: Cattaneo–Christov heat flux; Nanofluidics; Nanofluid and hybrid nanofluid; Curved surface; efficiency; Finite Element Method; Modified Fourier Law

1. Introduction

The study of nanofluid (NF) is significant in mathematics, engineering, physics, and materials discipline. Nanofluid refers to a type of fluid that contains tiny particles of a solid material, typically less than 100 nanometers in size, which are dispersed evenly throughout a liquid medium. These solid particles are often made of materials such as metals, oxides, or carbon-

based compounds, and they can enhance the thermal and mechanical properties of the fluid. The addition of nanoparticles to a fluid can increase its thermal performance, which is the ability to transfer heat, as well as its convective heat transfer coefficient, which measures the rate of heat transport through the fluid due to its motion. This makes NFs potentially useful in widespread applications, including heat transfer in electronic devices, conserving systems, and industrial processes. Nanofluids are still an vigorous area of investigation, and scientists are continuing to explore their properties and potential applications. However, challenges remain in terms of the cost of production, stability of the nanoparticles in the fluid, and potential health and safety concerns associated with handling nanoparticles.

The evolution of nanofluid (NF) innovation is a critical topic in arithmetic, manufacturing, physics, and environmental science. Engineers and researchers slog hard to effectively transmit applicable knowledge of the heat transport appliance in nanofluids for the bulk of actual uses. Chips, freezers, hybrid-power engines, food development, heat reservoirs, and more applications rely on NF. The notion of NF was initially established by Choi et al. [1]. Buongiorno [2] offered a theoretic form of the nanostructures and recognized that this vital mechanism sanctions us with massive flexibility in enlightening the thermal assets. Alzahrani et al. [3] investigated the influence of thermal and heaty analysis of Casson nanofluid subject to the suction through plane wall flow. Madhukesh et al. [4] studied the buoyancy effect in dual flow using titanium oxide, Ag, and Al_2O_3 using water as a host fluid over contracting sheet. The exponential flow of hybrid nanofluid with inters heat using Cattaneo–Christov heat model was inspected by Nagapavani et al. [5]. Haq et al. [6] explored the influence of hybrid nanofluid utilizing different geometries under the influence of homogeneous and heterogeneous reactions. Algehyne et al. [7] examined the Blasius and Sakiadis movement of Casson hybrid nanofluid across a moving plate. Ahn et al. [8] scrutinized the stability and convergence of hybrid nanofluid (HNF) over rotating disc.

Similarly, the entropy generation using magnetic dipole Casson nanofluid with nonlinear thermal effect was reported by Ragupathi et al. [9]. Sandeep and Ashwinkumar [10] used Carreau fluid to investigate the magnetized motion of a stagnation point movement (SPM) including nano sized materials. Similarly, Sandeep et al. [11] reflected the consequence of HNF on heat energy. Samrat et al. [12] inspected the heat transmission rate (HTR) in HNF and provided concurrent solutions. Yasmin et al. [13] reported the stability of three-dimensional Sutterby nanofluid over contracting surface. Alqahtani et al. [14] investigated the MHD flow over surved sheet with

stability of micropolar fluid with thermal impact. Rasheed et al. [15] gave the analytical solutions for MHD nanofluid with thermal and chemical reaction. Yasmin et al. [16] explored the stability of nanofluid with heat transfer analysis with dual solutions. [17-26] investigated certain NF uses for several physical challenges.

Boundary layer flow is a phenomenon in fluid mechanics that follows when a fluid streams above a solid surface. In this type of flow, the fluid in direct contact with the solid surface moves at the same speed as the surface, while fluid flow acceleration fluid far away from the sheet steadily growths till it touches the free stream acceleration. The boundary-layer thickness (BLT) depends on numerous features, comprising the viscosity, density, fluid velocity, and the irregularity of the solid surface. In general, the BLT upsurges with distance from the sheet and can be classified into three regions: laminar, transitional, and turbulent. Boundary layer flow has significant uses in countless fields, including aerodynamics, hydro-dynamics, and heat transmission.

Carbonization, warming system development, nuclear reactor safety, diffusion heating systems, solar dams, photovoltaic energy collectors, photochemical processes, and numerous other industrial processes use convection boundary layer liquid over an expanded surface subjected to thermal energy. Many design tasks arise at extremely high temperatures, rendering knowledge of heat transport through radiation crucial for the development of associated tools. Nuclear energy plants, boilers, and other engine machinery for airliners, spaceship, satellites, and communications satellites are examples of such industrial fields. Many scholars explored the outcome of thermal non-linearity on the thermal characteristics of both Newtonian and non-Newtonian fluids across an extended sheet in the context of magnetized Jeffrey NF. Pantokratoras [27] examined the impact of the Rosseland theory on the naturally occurring convection along a vertically homogenous plate to the primary time in his work using an innovative radiation component termed film radioactivity factor. Cortell [28] studied the mobility of liquids and an erratic thermal radiation transport along an extended surface. Mushtaq et al. [29] examined solar-induced stochastic radioactive heat exchange in a Williamson fluid. Laxmi et al. [30, 31] inspected the outcome of radiating heat and a uniformly generated electric field on 3D NF movement with thermophoresis and Brownian motion stimuli. The free-slip criterion is unsatisfactory for a large number of dynamic fluids since some polymer melts commonly exhibit tiny wall slip that is governed by a quadratic and predictable relationship among slip velocity and

suction. When the fluid is particle, such as suspensions, suspensions, spumes, and polymeric purposes, partial slip might occur at the stretched sheet's border. Slip characteristics can arise in a number of manufacturing procedures along the borders of tubes, walls, curved surfaces, and so on. The Navier velocity slip criteria is a popular way to investigate slide occurrences. A boundary layer slip flow problem develops when improving artificial cardiac valves and internal chambers. The authors have developed theoretical and computational methods for boundary layer motion and heat transfer generated by an extended surface. Aziz [32] investigated the magnetized mobility using NF passing through an absorbent layer having slip influence. Pantokratoras et al. [33] investigated the HNF in an irregular laminar, aluminium water-soluble micro-channel stream on a smooth surface using a 2D electrically conductive slippage action. Goyal et al. [34] conducted an in-depth investigation of the mixed-convective flow as well as heat transfer of a UCMF (Upper-Convected Maxwell Fluid) passing through an absorbing flexible plane. Nadeem et al. [35] used Lie group transformations and computational methodologies to study the inspiration of slip in magnetohydrodynamic natural convection flow of tiny particles fluid over a moveable surface.

Many investigations have been directed to explore the parameters that control the nanoparticle's conflict to heat transport by convection. It is interested to footnote that FL (Fourier law) was deliberated as a usual for heat distribution but after that it is pragmatic, it is not lawful in various phenomena owing to early disturbance which overcomes during the practice. Nanoparticles movement is stimulated by Brownian motion and thermophoresis. Frequent studies appeared to reveal that the development of the motile microbes in nanofluid movement [36]. The FL model is implemented to analyse the dispute of heat diffusion, whereby was tough to understand. Subsequently, Cattaneo's and Later Christov, a improved version of the FL was produced and functional to deliberate and scrutinize the matter of heat transmission over a extending sheet [37–41]. The unsteady slip stream of nanofluid beside a flat cylinder reveals that incentive energy has a momentous influence on nanoparticle motion inside the conventional liquids [39-41]. Temperature and concentration characteristics are unaffected via bio-convection factor [42- 46], whereas the buoyancy parameter has an impact on the density and velocity of fluid. As a result of the mass slip, enhances the density, temperature, fluid flow, whereas it modestly lowers the particle concentration [47]. The topic of this research is the bio-convection tool through a contracted cylinder. Recent research on the mechanics of nanofluids in various configurations,

Cattaneo used the thermal moderation in the Fourier model. This is monitored by Christov who suggested replacing the Oldroyd Upper Convective Derivatives (OUCD) with time. The Maxwell nanofluid flow through a stretched surface with C–C using homotopy analysis method (HAM) method.

Grounded on the specified literature, in the existing study, this study investigates the HN movement past a stretched curve enclosing heat transfer. Nanoparticles like Cu and CuO are emerged in EG using a base fluid. At the boundary the slip effect is observed using Modified Fourier Law (MFL). The flow characteristics are examined by assign numerical values to the physical parameters. The novelty of the problem is to examine the stability of dusty-hybrid nanofluid with slip effect. The leading equations are converted to ODEs through appropriate transformation and numerically computed via Runge-Kutta order four method (RK4) method. The influences of the factors are deliberated graphically. Additionally, for confirmation the present work is compared with the previous.

2. Mathematical Modulation

Consider two-dimensional movement of an incompressible nanofluid and HNF with magnetic influence through exponentially extended curved surface with non-linear heat radiation. Laminar, time-independent fluid motion is observed. Let, (r, s) is the frame of reference in which r-axis is normal to flow and s-axis is parallel to the flow direction. Let d signifies the radius of the circle. The mentioned geometry is stretched with a rate of $u = a_1 e^{\frac{s}{l}}$ alongside the surface way $(a_1, l \succ 1)$ where A and L are initial stretching rate and reference length, respectively. As shown in Fig. 1, the magnetic effect is taken in radial direction. The MFL is applied to analyses the heat mechanism.

The basic flow equations for the current models are explained below [47]:

2.1 For nanoliquid:

$$\frac{\partial}{\partial r}\{(R+r)v\} + R\frac{\partial u}{\partial s} = o, \tag{1}$$

$$\frac{u^2}{r+R} = \frac{1}{\rho_{hnf}}\frac{\partial p}{\partial r}, \tag{2}$$

$$v\frac{\partial u}{\partial r}+\left(\frac{Ru}{r+R}\right)\frac{\partial u}{\partial s}+\frac{uv}{r+R}=-\left(\frac{1}{\rho_{hnf}}\frac{R}{r+R}\right)\frac{\partial p}{\partial s}+ \frac{\mu_{hnf}}{\rho_{hnf}}\left(\frac{\partial^2 u}{\partial r^2}+\frac{1}{r+R}\frac{\partial u}{\partial r}-\frac{u}{\left(r+R\right)^2}\right)-\frac{KS}{\rho_{hnf}}\left(u_p-u\right), \tag{3}$$

$$\left(\rho C_p\right)_{hnf}\left(v\frac{\partial T}{\partial r}+\frac{Ru}{r+R}\frac{\partial T}{\partial s}\right)=-\nabla.q+\frac{\rho pC_{pf}}{\tau T}\left(T_p-T\right)+\frac{\rho pC_p}{\tau_v}\left(u_p-u\right)^2, \tag{4}$$

$$q+\lambda_\Gamma\left(V.\nabla q-q.\nabla V+\left(\nabla.V\right)q\right)=K^o\nabla T. \tag{5}$$

For incompressible flow

$$\nabla.V=0 \tag{6}$$

Eq. (5) becomes:

$$q+\lambda_\Gamma\left(V.\nabla q-q.\nabla V\right)=K^o\nabla T \tag{7}$$

Heat equations becomes:

$$v\frac{\partial T}{\partial r}+\frac{Ru}{r+R}\frac{\partial T}{\partial s}=\frac{K^o}{\left(\rho C_p\right)_{hnf}}\left[\begin{array}{l}\frac{\partial^2 T}{\partial r^2}+\frac{1}{r+R}\frac{\partial T}{\partial r}+\left(\frac{R}{r+R}\right)^2\frac{\partial^2 T}{\partial s^2}- \\ \lambda_\Gamma\left(u^2\left(\frac{R}{r+R}\right)^2\frac{\partial^2 T}{\partial s^2}\right)+v^2\frac{\partial^2 T}{\partial r^2}+\left(v\frac{\partial v}{\partial r}+u\frac{\partial v}{\partial s}+\frac{R}{r+R}\right)\frac{\partial T}{\partial r} \\ +\frac{R}{r+R}v\frac{\partial u}{\partial s}\left(\begin{array}{l}u\frac{\partial u}{\partial s}\left(\frac{R}{r+R}\right)^2\frac{\partial u}{\partial s}+\left(\frac{R}{r+R}\right)v\frac{\partial u}{\partial s}\frac{\partial T}{\partial s}+ \\ 2v\frac{R}{r+R}v\frac{\partial^2 T}{\partial r\partial s}\end{array}\right)\end{array}\right] + \frac{\rho pC_{pf}}{\left(\rho C_p\right)_{hnf}\tau T}\left(T_p-T\right)+\frac{\rho pC_{pf}}{\left(\rho C_p\right)_{hnf}\tau_v}\left(u_p-u\right)^2, \tag{8}$$

1.1.For dusty liquid [47]:

$$\frac{\partial}{\partial r}\left\{\left(R+r\right)v_p\right\}+R\frac{\partial u_p}{\partial s}=0, \tag{9}$$

$$v_p\frac{\partial u_p}{\partial r}+\frac{Ru_p}{r+R}\frac{\partial u_p}{\partial s}+\frac{u_pv_p}{r+R}=\frac{KS}{\rho_p}\left(u_p-u\right)' \tag{10}$$

$$v_p\frac{\partial T_p}{\partial r}+\frac{Ru_p}{r+R}\frac{\partial T_p}{\partial s}=\frac{C_p}{C_m\tau_T}\left(T_p-T\right), \tag{11}$$

Owing to constraints

$$u\left|_{r=0}=a_1e^{\frac{s}{l}}+\lambda_1\left(\frac{u}{r+R}-\frac{\partial u}{\partial r}\right|_{r=0}\right)+\left(\lambda_2\frac{\partial^2 u}{\partial r^2}\right|_{r=0}-\frac{u}{(r+R)^2}+\frac{1}{r+R}\frac{\partial u}{\partial r}\left|_{r=0}\right.\right), \tag{12}$$

$$\begin{aligned} &T\left|_{r=0}=T_m, k_{hnf}\frac{\partial T}{\partial r}\right|_{r=0}=\rho_{hnf}\left(\lambda+C_s\right)\left(T_m-T_o\right)v\left(s,0\right),\\ &u\left|_{r\to\infty}\to 0, u_p\right|_{r\to\infty}\to 0, v_p\left|_{r\to\infty}\to v, \frac{\partial u}{\partial r}\right|_{r\to\infty}\to 0, T\left|_{r\to\infty}\to T_\infty\right.\end{aligned} \tag{13}$$

The thermal physical features for NF are

$$\mu_{nf}=\frac{\mu_f}{\left(1-\phi\right)^{2.5}}a_{1nf}=\frac{k_{nf}}{\left(\rho C_p\right)_{nf}}, \tag{14}$$

$$\rho_{nf}=\left(1-\phi\right)\rho_f+\phi\rho_s, \left(\rho C_p\right)_{nf}=\left(1-\phi\right)\left(\rho C_p\right)_f+\phi\left(\rho C_p\right)_s, \tag{15}$$

$$\frac{k_{nf}}{k_f}=\frac{\left(k_s-2k_f\right)-2\phi\left(k_f-k_s\right)}{\left(k_s+2k_f\right)+2\phi\left(k_f-k_s\right)} \tag{16}$$

The HNF thermo-physical features are followed as:

$$\mu_{nf}=\mu_f\left(1-\phi_1\right)^{-2.5}\left(1-\phi_2\right)^{-2.5}, \tag{17}$$

$$D_4=\left(\rho C_p\right)_{hnf}=\left(\rho C_p\right)_{s_2hnf}\phi_2-\left(\phi_2-1\right)\left\{\left(1-\phi_1\right)\left(\rho C_p\right)_f+\left(\rho C_p\right)_{s_1}\phi_1\right\}. \tag{18}$$

$$\rho_{hnf}=\left(1-\phi_2\right)\left\{\left(1-\phi_1\right)\rho_f+\phi_1\rho_{s1}\right\}+\rho_{s2}\phi_2, \tag{19}$$

$$\begin{aligned} &\frac{k_{hnf}}{k_f}=\frac{k_{bf}\left(n-1\right)+k_{s2}-\left(n-1\right)\left[k_{bf}-k_{s2}\right]\phi_2}{k_{bf}\left(n-1\right)+k_{s2}+\left[k_{bf}-k_{s2}\right]\phi_2},\\ &\frac{k_{bf}}{k_f}=\frac{k_{s1}+\left(n-1\right)k_f-\left(n-1\right)\left[k_f-k_{s1}\right]\phi_1}{k_{s1}+\left(n-1\right)k_f+\left[k_f-k_{s1}\right]\phi_1},\end{aligned} \tag{20}$$

3. **Introducing new transformation**

4. The equivalent PDEs for DNF and DHNF are altered to ODEs by presenting the succeeding transformation [47]:

$$\eta = \sqrt{\frac{a_1}{2l\upsilon f}} r e^{s/2l},\ p = \rho_f a_1^2 e^{2s/l} P(\eta), \theta(\eta) = \frac{T - T_m}{T_\infty - T_m}, \theta_p(\eta) = \frac{T_p - T_m}{T_\infty - T_m},$$

$$u = a_1 e^{s/l} f'(\eta), v = -\frac{R}{r+R}\sqrt{\frac{a_1 \upsilon_f}{2l}} e^{s/2l}\left(f'(\eta) + \eta f'(\eta)\right), \tag{21}$$

$$u_p = a_1 e^{s/l} f'(\eta), v = -\frac{R}{r+R}\sqrt{\frac{a_1 \upsilon_f}{2l}} e^{s/2l}\left(f'(\eta) + \eta f'(\eta)\right),$$

4.1.**For nanoparticles fluid**

$$\frac{\rho_f}{\rho_{hnf}} P' = \frac{f'^2}{\eta + K_p} \tag{22}$$

$$\frac{\rho_f}{\rho_{hnf}} \frac{2k}{\eta + k} P = \frac{\mu_{hnf}/\mu_f}{\rho_{hnf}/\rho_f}\left(f''' - \frac{f'}{\left(K_p + \eta\right)^2} + \frac{f''}{\eta + K_p}\right) - \frac{K_p f'^2}{\eta + K_p} + \frac{K_p f f''}{K_p + \eta} + \frac{K_p f f'}{\left(K_p + \eta\right)^2} + \frac{I_m B_v}{\rho_{hnf}}\left(F' - f'\right) \tag{23}$$

$$\frac{1}{P_r}\frac{k_{hnf}}{K_p}\left(\theta + \frac{1}{\eta + K_p}\theta\right) + D_4\left[\frac{K_p}{\eta + K_p} f\theta - \varepsilon_{Ther}\left(\frac{K_p^2}{\left(\eta + K_p\right)^2}\left(f\theta'' + f f'\theta'\right) - K_p^2 f^2 \theta'\right)\right] + M_d B_\gamma\left(\theta_p - \theta\right) + M_d B_v E_C\left(F' - f'\right) = 0, \tag{24}$$

1.1.**For Dusty fluid flow:**

$$\frac{K_p}{K_p + \eta} FF'' - \frac{K_p}{\eta + K_p} F'^2 + \frac{K_p}{\left(\eta + K_p\right)^2} F'F + B_v\left(f' - F'\right) = 0, \tag{25}$$

$$\frac{K_p}{K_p + \eta} F\theta_p - \gamma B_\gamma\left(\theta_p - \theta\right) = 0, \tag{26}$$

Corresponding to the altered boundary conditions:

$$D_2 Prf(0) + \frac{k_{hnf}}{k} M\theta'(0) = 0, \quad f'(0) - 1 - L_0\left(f''(0) - \frac{f'(0)}{K_p}\right) - L_1\left(f'''(0) - \frac{f''(0)}{\eta + K_p} - f''(0) - \frac{f'(0)}{\left(\eta + K_p\right)^2}\right) = 0, \tag{27}$$

$\theta(0) = 1, \theta(\eta) \to 0, \theta_p(\eta) \to 0, as\ \eta \to \infty$

Involved parameters are expressed as

$$K_p = R\sqrt{\frac{a}{2\nu_{fl}}}, B_\nu = \frac{1}{a_1 T_\nu}, \Pr = \frac{\nu f}{a_f}, B_\gamma = \frac{1}{a_1 T_T}, \varepsilon_{Ther} = a_1\lambda, M = \frac{C_P\left(T_m - T_0\right)}{\lambda + C_s\left(T_m - T_0\right)}$$
$$E_c = \frac{a_1^2 e^{2s/l} 2l}{C_P\left(T_\infty - T_m\right)}, M_d = \frac{mS}{\rho_P}, Sc = \frac{V_f}{D}, L_0 = \lambda_1\sqrt{\frac{a_1}{2\nu_f l}}, L_1 = \lambda_2\sqrt{\frac{a_1}{2\nu_f l}}. \quad (28)$$

From equations (22) and (23) [47]

$$f''' + \frac{2f'''}{\eta + K_p} - \frac{f''}{\left(\eta + K_p\right)^2} + \frac{f'}{\left(\eta + K_p\right)^3} + D_1 M_d B_\nu + \frac{1}{\left(\eta + K_p\right)}\left(F' - f'\right)$$
$$+ D_1 D_2\left\{\frac{K_p}{\left(\eta + K_p\right)^2}\left(f'^2 - ff''\right) - \frac{K_p}{\left(\eta + K_p\right)}\left(f'f'' - ff'''\right) - \frac{K_p}{\left(\eta + K_p\right)^3} ff'\right\} = 0, \quad (29)$$

The surface drag force $\left(C_f\right)$,

$$C_f = \frac{T_{rX}}{\frac{1}{2}\rho q_w^2}. \quad (30)$$

where,

$$T_{rX} = \mu_{nf}\left(\frac{\partial u}{\partial r} - \frac{u}{r + R}\right)_{r=0}. \quad (31)$$

After Simplification we get,

$$C_f\sqrt{\mathrm{Re}_s} = \frac{1}{D_1}\left(f''(0) - \frac{f'(0)}{K_p}\right). \quad (32)$$

Here, Re_s denotes the local Reynolds Number (LRN).

5. Error analysis

The results produced by the Finite Element Method (FEM) are generally quite accurate with regard to most differential equations. However, since its outcomes are founded on numeric error assessments, considerable error is exceptionally small. It is frequently helpful to scrutinize conclusions by concerning an explanation that was generated with Work Precision (WP) greater than the Default Machine Precision (DMP). For this purpose, estimations is done through FEM procedure with the DWP, and the error is figured out using FEM via WP-22. Since, errors are normally minor, therefore it is beneficial to evaluate them on scale [10] (logarithmic scale).

We intended the error approaches to various physical variables involved in the suggest problem via graphically. We carried out an evaluation of errors to confirm the validity of the procedure before performing physical measurements. Figures 2-8 were created for this analysis. The lowest possible error rate (10–30) is preserved throughout each calculation in the FEM process. reducing the total mean squared residual error by utilizing the FEM tool in Mathematica. To

detect error for different orders of estimate, several iterations is done for the different magnitude of Kp, pi and ϕ_2 fixing $L_0 = 1.2, L_1 = 1.2, B_v = 1.3, M = 0.2$ and $M_d = 1.3$. Figures 2-4 demonstration the maximum ASQE for numerous values of Kp by several estimate orders. It is perceived that the designated values of Kp to display the inspiration on DPV and DPT is noteworthy. MSRE and TMSRE are displayed in Fig. 5, when $\phi_2 = 0.2$ the TASRE and ASRE drop as the instruction of approximation upsurges, but for $\phi_2 = 0$, the error is melodramatically abridged as associated with the situation for $\phi_2 = 0.2$, as realized in Fig. 5. Thus, when $\phi_2 = 1$, the imprecision growths as demonstrated in Figure 8.

6. Analysis and results

In this research, we look at the NF and HN across a surface that curves with dust particles to illustrate how melting heat and SoS at the border affect the results. The modeled PDEs are similarly transformed into convectional ordinary differential equations and subsequently solved computationally with FEM utilizing MATHEMATICA SOFTWARE. This section uses graphs and tables to examine the effects of different dimensionless factors on the flow field, dust phase velocity (DPV), heat field, DPT, and physical measurements of concern like SF. Also confirmation is debated with the earlier work. The link between the fluid's DPV and the curve of the surface that curves (CCS) is examined in Figure 9. It should be noted that once the CCS is raised, the fluid's DPV is improved. As a consequence, decreasing curved sheeting radius comes across a smaller surface area of interaction, and flowing participation eventually entails the least conflict. The higher liquid speed is evident as a result. Figure 10 illustrates a different tendency because of the DPT in an analogous way. As opposed to a movement in CCS, the rate of heat conduction within the liquid via the sheet is slightly slower. As an outcome, the DPT is thought to be declining. It is crucial to understand that HN produces outcomes that are superior to nano-liquid streams.

The purpose of Figures 11 and 12 is to examine the impact of the volume of a solid fraction ϕ_2 to the liquid's velocity for both phases $f'(\eta)$ and $F'(\eta)$. It is noted that the fluid's motion $f'(\eta)$ exhibits improved efficiency near to the surface while reducing ability farther from the border is shown for greater assessments of ϕ_2 . For dust liquid $F'(\eta)$, boosting events are also seen (Figure 12). Again, this demonstrates the HNF potential.

The heat transmission increases as a consequence of a rise in the ability to conduct the heat of nanotechnology particles, which in turn raises the fluid's temperature (Figure 13) across both HN and NF. In Figure 14, the liquid's DPT $\theta_p(\eta)$ is depicted for various ϕ_2 values. It is noted that the $\theta_p(\eta)$ decreases. In addition, it was evident that, in comparison to the HN, the measured percentages of tiny material that were present had the least impact on the copper-containing nanofluid owing to the lower estimated densities of the nanofluid. Additionally, the inclusion has the least impact on the copper-containing nanofluid.

The efficiency of the liquid dust stage heat for differentiating solid volumetric fraction data is shown in Figure 14. The ambient temperature of the fluid at the dust stage is thought to be dropping. Because of the lowered density predictions of the copper-based EG. It was also found that the EG NF was only marginally influenced by the penetration of ϕ_2 compared to the (CuCuO)-HN. The variance in $f'(\eta)$ for various values of the variables L_0 (first) and L_1 (second) is shown in Figures 15 and 16. This research shows that under both situations, there are increases in L_0, signs of a descending acceleration magnitude $f'(\eta)$, and increases in L_1 the velocity of the fluid.

The outcome of melting heat factor M on the flow field is seen in Figure 17. It follows that the number of liquid molecules with fluid dust speeds ascends towards larger M. This is due to the particle motion is more anchored, which eventually aids the fluid's speed. HN properties have a big role. Figures 18 and 19 show how different amounts of B_v and M_d on $F'(\eta)$ correspondingly. It is inspected that the DPV showing the declining behaviour with enhancing B_v and M_d.

Figure 20 is created for a range of values of ε_{Ther} (thermal relaxation time) on heat. A change in ε_{Ther} estimates indicate a lower temperature. The fluid's temperature has decreased as a result of the confinement type, which is shown by larger approximation of ε_{Ther}.

Figure 21 shows the significance of factors γ on DPT. The internal heat of the fluid rises with increasing values of γ. The outcome of the Eckert number Ec on the heat for conventional nanofluids and hybrid nanofluids is seen in Figure 22. A large heat change is seen with rising Ec values. Frictional heating brought on by an improvement in Ec is the cause of this heat buildup.

Thermo physical characteristics values for base fluid and Nanomaterial are given in Table1. Table 2 details the rationale of our results that are currently accessible. This table makes clear that the current results and the published study accord superbly [47]. Skin Friction (SF) variation is shown in Table 3 for analytical estimations of various parameters. According to growing estimates of $\phi_{2,}$ $L_{0,}$, and K_p. SF appears to grow. In contrast, an opposite trend is endorsed in the cases of L_1 and M in the numerical simulations of NF and HN, respectively.

7. Concluding remarks

This study involves the introduction of dust grains that are enclosed in Cu/EG (NF) and Cu-CuO/EG (HN) approaching modified FL via a curving surface having a slip mechanism. The statistical issue is resolved through the FEM approach, and the impacts of various components are illustrated against relevant profiles and in a structured manner in diagrams. The ND-Solve technique is used to validate the FEM. The comparison of the current work to earlier work and error assessment serves to corroborate the theoretical framework. When K_p is increased, it is seen that the $F'(\eta)$ is enhanced. For different values of $\phi_{2,}$, the behavior shown by $f'(\eta)$ and $F'(\eta)$ is reversed. The heat of the fluid drops in relation to the thermal relaxation coefficient. Comparable increasing and declining patterns can be seen in the velocity and thermal curves versus the curvature variable for both the liquids and dusty phases. The HN effectiveness is significantly higher compared to that exhibited by the traditional NF. The consequences of the first-order slip variable, the curved variable, and the pulling force contribution on the flow field, DPV, heat, and DPT all increase with time.

Data Availability statement: All the data is available within the manuscript.

Conflicts of Interest: The authors declare no conflict of interest.

References

[1] Choi, S.U. and Eastman, J.A. "Enhancing thermal conductivity of fluids with nanoparticles", (No. ANL/MSD/CP-84938; CONF-951135-29). IL (United States): Argonne National Lab.; (1995).

[2] Buongiorno, J. "Convective Transport in NFs", *Journal of Heat Transfer*, 128: pp.240-250 (2006).

[3] Alzahrani, H.A., Alsaiari, A., Madhukesh, J.K., et al. "Effect of thermal radiation on heat transfer in plane wall jet flow of Casson nanofluid with suction subject to a slip boundary condition", *Waves in Random and Complex Media*, pp.1-18 (2022).

[4] Madhukesh, J.K., Kumar, R.N., Khan, U., et al. "Analysis of buoyancy assisting and opposing flows of colloidal mixture of titanium oxide, silver, and aluminum oxide nanoparticles with water due to exponentially stretchable surface", *Arabian Journal of Chemistry*,16(4), p.104550 (2023).

[5] Nagapavani, M., Kanuri, V.R., Fareeduddin, M., et al. "Features of the exponential form of internal heat generation, Cattaneo–Christov heat theory on water- based graphene–CNT–titanium ternary hybrid nanofluid flow", *Heat Transfer*, 52(1), pp.144-161 (2023).

[6] Haq, I., Naveen K.R., Gill, R., et al. "Impact of homogeneous and heterogeneous reactions in the presence of hybrid nanofluid flow on various geometries", *Frontiers in Chemistry*, 10, p.1032805 (2022).

[7] Algehyne, E.A., Gamaoun, F., Lashin, M.M., et al. "Blasius and Sakiadis flow of a Casson hybrid nanofluid over a moving plate". *Waves in Random and Complex Media*, 2022, pp.1-18 (2022).

[8] Ahn, K., Suganya, S. and Muthtamilselvan, M. "Convergence and stability analysis on the rotating hybrid flow of Cu–Fe2O3/water", *Numerical Heat Transfer, Part B: Fundamentals*, 2023, pp.1-23 (2023).

[9] Ragupathi, E., Prakash, D., Muthtamilselvan, M. et al. "Entropy analysis of Casson nanofluid flow across a rotating porous disc with nonlinear thermal radiation and magnetic dipole", *International Journal of Modern Physics B*, 37(26), p.2350308 (2023).

[10] Sandeep, N and Ashwinkumar, G.P. "Impact of nanoparticle shape on magnetohydrodynamic stagnation-point flow of carreau nanoliquid: A comparative study", *Proc Inst Mech Eng Part E: J Process Mech Eng.*, 236(3), (2021).

[11] Sandeep, N., Ranjana, B., Samrat, S.P., et al. "Impact of nonlinear radiation on magnetohydrodynamic flow of hybrid NF with heat source effect", *Proc Inst Mech Eng Part E:* J Process Mech Eng. 236(4), 09544089211070667 (2022).

[12] Samrat, S.P., Ashwinkumar, G.P. and Sandeep, N. "Simultaneous solutions for convective heat transfer in dusty-nano-and dusty-hybrid nanoliquids", *Proc Inst Mech Eng Part E: J Process Mech Eng.*, 236(2), 09544089211043605 (2021).

[13] Yasmin, H., Zeeshan, Z., Alshehry, A.S., Ganie, A.H. and Shah, R., A theoretical stability of mixed convection 3D Sutterby nanofluid flow due to bidirectional stretching surface. Scientific Reports, 2023, 13(1), p.22400.

[14] Alqahtani, A.M., Zeeshan, Khan, W., Alhabeeb, S.A. and Khalifa, H.A.E.W., 2023. Stability of magnetohydrodynamics free convective micropolar thermal liquid movement over an exponentially extended curved surface. Heliyon, 9(11).
[15] Rasheed, H.U., Zeeshan, Islam, S., et al. "Analytical evaluation of magnetized nanofluid flow in a stagnation point with chemical reaction and nonlinear radiation effect configured by an extended surface", *ZAMM - Journal of Applied Mathematics and Mechanics/Zeitschrift für Angewandte Mathematik und Mechanik*, 103(2), (2023).
[16] Yasmin, H., Alshehry, A.S., Zeeshan, et al. "Stability of non-Newtonian nanofluid movement with heat/mass transportation passed through a hydro magnetic elongating/contracting sheet: multiple branches solutions", Scientific Reports, 13(1), pp.17760 (2023).
[17] Ashwinkumar, G.P. "Heat and mass transfer analysis in unsteady MHD flow of aluminum alloy/silver-water nanoliquid due to an elongated surface", *Heat Transfer*. 50(2): pp.1679-1696 (2021).
[18] Ashwinkumar, G.P, Samrat, S.P, Sandeep, N. "Convective heat transfer in MHD hybrid NF flow over two different geometries", *Int Commun Heat Mass Transfer*. 127, pp.05563 (2021).
[19] Samrat, S.P., Ashwinkumar, G.P. and Sandeep, N. "Simultaneous solutions for convective heat transfer in dusty-nano-and dusty-hybrid nanoliquids", *Proc Inst Mech Eng Part E: J Process Mech Eng*.236(2), pp.09544089211043605 (2021).
[20] Tlili. I., Nabwey, H.A., Samrat, S.P. et al. "3D MHD nonlinear radiative flow of CuO-MgO/methanol hybrid NF beyond an irregular dimension surface with slip effect", *Sci Rep*. 10(1), pp.1-14 (2020).
[21] Alotaibi, H., Althubiti, S., Eid, M.R., et al. "Numerical treatment of MHD flow of casson NF via convectively heated non-linear extending surface with viscous dissipation and suction/injection effects", *Comput Mater Continua*. 66(1), pp.229-245 (2020).
[22] Yu, B., Ramzan, M., Riasat. S., et al. "Impact of autocatalytic chemical reaction in an Ostwald-de-Waele NF flow past a rotating disk with heterogeneous catalysis", Sci Rep. 11(1), pp.1-17 (2021).
[23] Shaheen, N., Ramzan, M., Alshehri, A., et al. "Soret–Dufour impact on a three-dimensional Casson NF flow with dust particles and variable characteristics in a permeable media", Sci Rep. 11(1), pp.1-21 (2021).
[24] Bilal, M., Ramzan, M., Mehmood, Y., et al. "An entropy optimization study of non-Darcian magnetohydrodynamic Williamson NF with nonlinear thermal radiation over a stratified sheet", *Proc Inst Mech Eng Part E: J Process Mech Eng*., 235(6), pp.1883–1889 (2021).
[25] Liu, C, Khan, M.U., Ramzan, M., et al. "Nonlinear radiative Maxwell NF flow in a Darcy–Forchheimer permeable media over a stretching cylinder with chemical reaction and bioconvection", *Sci Rep.* 11(1), pp.1-21 (2021).
[26] Bashir, S., Ramzan, M., Chung, J.D., et al. "Analyzing the impact of induced magnetic flux and Fourier's and Fick's theories on the Carreau-Yasuda NF flow", *Sci Rep*. 11(1), pp.1-18 (2021).
[27] Pantokratoras, A. "Natural convection along a vertical isothermal plate with linear and non-linear Rosseland thermal radiation", *International journal of thermal sciences*, 84, pp.151-157 (2014).
[28] Cortell, R. "Fluid flow and radiative nonlinear heat transfer over a stretching sheet", *Journal of King Saud University-Science*, 26 (2), pp.161-7 (2014).
[29] Mushtaq, A., Mustafa, M., Hayat, T. et al. "Nonlinear radiative heat transfer in the flow of NF due to solar energy: A numerical study", *Journal of the Taiwan Institute of Chemical*

Engineer, 45(4), pp.1176-83 (2014).
[30] Laxmi, T.V., Shankar, B. "Effect of nonlinear thermal radiation on boundary layer flow of viscous fluid over nonlinear stretching sheet with injection/suction", *Journal of Applied Mathematics and Physics*, 4(2), pp.307-19 (2016).
[31] Shehzad, S.A., Hayat, T., Alsaedi, A. et al. "Nonlinear thermal radiation in three-dimensional flow of Jeffrey NF: a model for solar energy", *Applied Mathematics and Computation*. 248, pp.273-86 (2014).
[32] Aziz A. A similarity solution for laminar thermal boundary layer over a flat plate with a convective surface boundary condition. Communications in Nonlinear Science and Numerical Simulation. 2009;14(4):1064-8.
[33] Pantokratoras, A., Fang, T. "Sakiadis flow with nonlinear Rosseland thermal radiation", *Physica Scripta*, 87(1), pp.015703 (2012).
[34] Goyal, M., Bhargava, R. "Boundary layer flow and heat transfer of viscoelastic NFs past a stretching sheet with partial slip conditions", *Applied Nanoscience*, 4(6), pp.761-7 (2014).
[35] Chandran, P., Sacheti, N.C. and Singh, A.K. "Natural convection near a vertical plate with ramped wall temperature", *Heat Mass Transfer*, 41, pp.459-464 (2005).
[36] Akbar, N.S. and Khan, Z.H. "Magnetic field analysis in a suspension of gyrotactic microorganisms and nanoparticles over a stretching surface", *J Magn Magn Mater*, 410, pp.72–80 (2014).
[37] Chakraborty, T., Das, K. and Kundu, P.K. "Framing the impact of external magnetic field on bioconvection of a nanofluid flow containing gyrotactic microorganisms with convective boundary conditions", *Alexandria Eng J.*, 57(1), pp.61-71 (2018).
[38] Acharya, N., Das, K. and Kundu, P.K. "Framing the effects of solar radiation on magneto-hydrodynamics bioconvection nanofluid flow in presence of gyrotactic microorganisms", *J Mol Liq*., 222, pp.28-37 (2016).
[39] Uddin, M.J., Yasser, A.O., Bég. A. et al. "Numerical solutions for gyrotactic bioconvection in nanofluid-saturated porous media with Stefan blowing and multiple slip effects", *Comput Math Appl.*, 72 (10), pp.2562–81 (2016).
[40] Tausif, S.M., Das, K. and Kundu, P.K. "Multiple slip effects on bioconvection of nanofluid flow containing gyrotactic microorganisms and nanoparticles", *J Mol Liq* ., 220, pp.518–26 (2016).
[41] Aldabesh, A., Khan, S.U., Habib, D. et al. "Unsteady transient slip flow of Williamson nanofluid containing gyrotactic microorganism and activation energy", *Alexandria Eng J.*, 59 (6), pp.4315–28 (2020).
[42] Haq, F., Kadry, S. and Chu, Y.M. et al. "Modeling and theoretical analysis of gyrotactic microorganisms in radiated nanomaterial Williamson fluid with activation energy", *J Mater Res Technol.*, 9(5), pp.10468–77 (2020).
[43] Hussain, A. and Malik, M.Y. "MHD nanofluid flow over stretching cylinder with convective boundary conditions and Nield conditions in the presence of gyrotactic swimming microorganism: A biomathematical model", *Int Commun Heat Mass Transfer*, 126: pp.105425 (2021).
[44] Shi, Q.H., Hamid, A., Khan, M.I. et al. "Numerical study of bio-convection flow of magneto-cross nanofluid containing gyrotactic microorganisms with activation energy", *Scientific Reports*, 11, pp.16030 (2021).
[45] Yusuf, T.A., Mabood, F., Prasannakumara, B.C. et al. "Magneto-bioconvection flow of

Williamson nanofluid over an inclined plate with gyrotactic microorganisms and entropy generation", *Fluids*, 6(3), pp.109 (2021).
[46] Reddy, P.S. and Sreedevi P. "Impact of chemical reaction and double stratification on heat and mass transfer characteristics of nanofluid flow over porous stretching sheet with thermal radiation", *Int J Ambient Energy*; 43(1), pp.1-11 (2020).
[47] Ahmed, N., Saba, F., Khan, U., et al. "Nonlinear thermal radiation and chemical reaction effects on a (Cu-CuO)/NaAlg hybrid nanofluid flow past a stretching curved surface", *Processes*, 7(12), pp.962-24 (2019).

Biographies

Zeeshan earned his M.Sc. and M.phil degree from Quaid-e-Azam University, Islamabad and the Ph.D. degree from Abdul Wali Khan university, Mardan, KP, Pakistan. He is currently an Assistant Professor in mathematics with Bacha Khan University Charsadda, KP, Pakistan. He has published 90 articles in good impact factor journals and has participated in national conference. His research interests include magnetohydrodynamic, nano fluid, heat transfer, hall effect, electrohydrodynamic, thin film, and heat exchangers.

WARIS KHAN received his educational degrees as follows: M.Sc. degree from Quaid-e-Azam University, Islamabad, Pakistan. M.S. degree from COMSATS University Abbottabad, KP, Pakistan. Ph.D. degree from Islamia College University, Peshawar, KP, Pakistan. He currently holds the position of Lecturer of Mathematics at Hazara University, Mansehra, KP, Pakistan. He has a prolific academic record with 94 articles published in high-impact factor journals, along with active participation in national conferences. His research expertise spans various areas including magnetohydrodynamics, nanofluids, heat transfer, hall effect, electrohydrodynamics, thin films, and heat exchangers.

Maryam Redn ALmutiri received the MSc. degree from the Faculty of Science, Qassim University, Saudi Arabia. She is recently attached with the Department of Mathematics, College of Science and Arts, Qassim University, Dariyah, Saudi Arabia, for research projects. She has two publications in SCI journals. Her research interests include Pure & Applied Mathematics.

Badria Almaz Ali Yousif received the Ph.D. degree from the Faculty of Science, Baghat Alruda University, Sudan. She is recently attached with the Department of Mathematics, College of Science and Arts, Qassim University, Buraydah, Saudi Arabia, for research projects. She has published more than 10 publications in SCI journals. Her research interests include Game Theory, and Multi-objective Programming.

ABEER A. SHAABAN received the Ph.D. degree from the Faculty of Education, Ain Shams University, Cairo, Egypt. She is a Teacher in Mathematical Subjects (Computational Fluids). She is recently attached with the Mathematics Department the Faculty of Education, Ain Shams University, Cairo, Egypt, as Lecturer. She is also attached with the Department of Management Information Systems, College of Business Management, Qassim University, Ar Rass, Saudi Arabia, as Assistance Professor. Her research interests include, Fluid Flow, Computational Fluid Dynamics, Fluid Mechanics, Heat & Mass Transfer, Nano-fluids, Numerical Simulation, Numerical Analysis.

Figure1. Flow geometry.

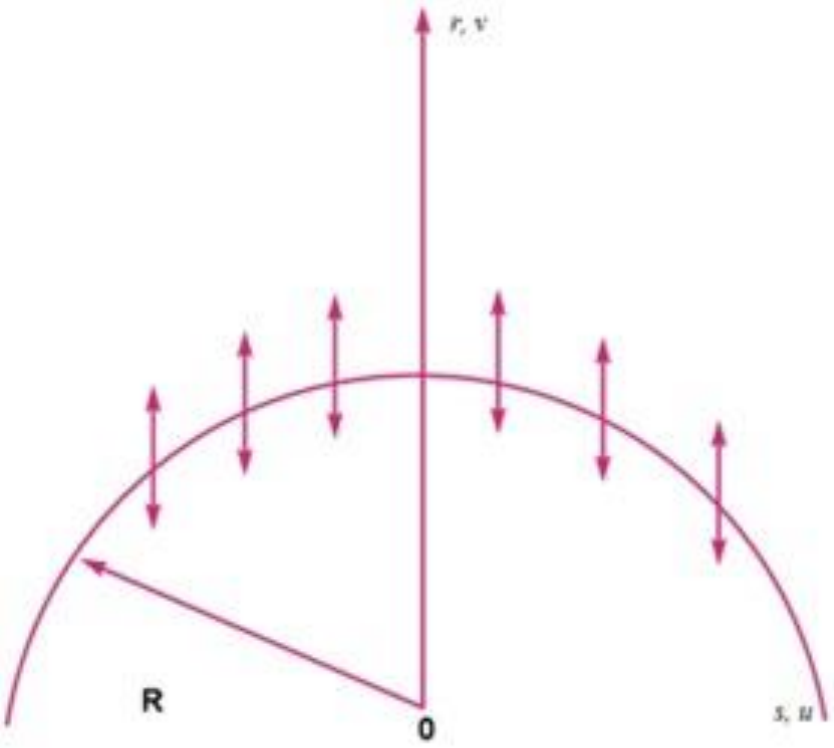

Figure 2(a-b). Error estimation for $K_p = 2$

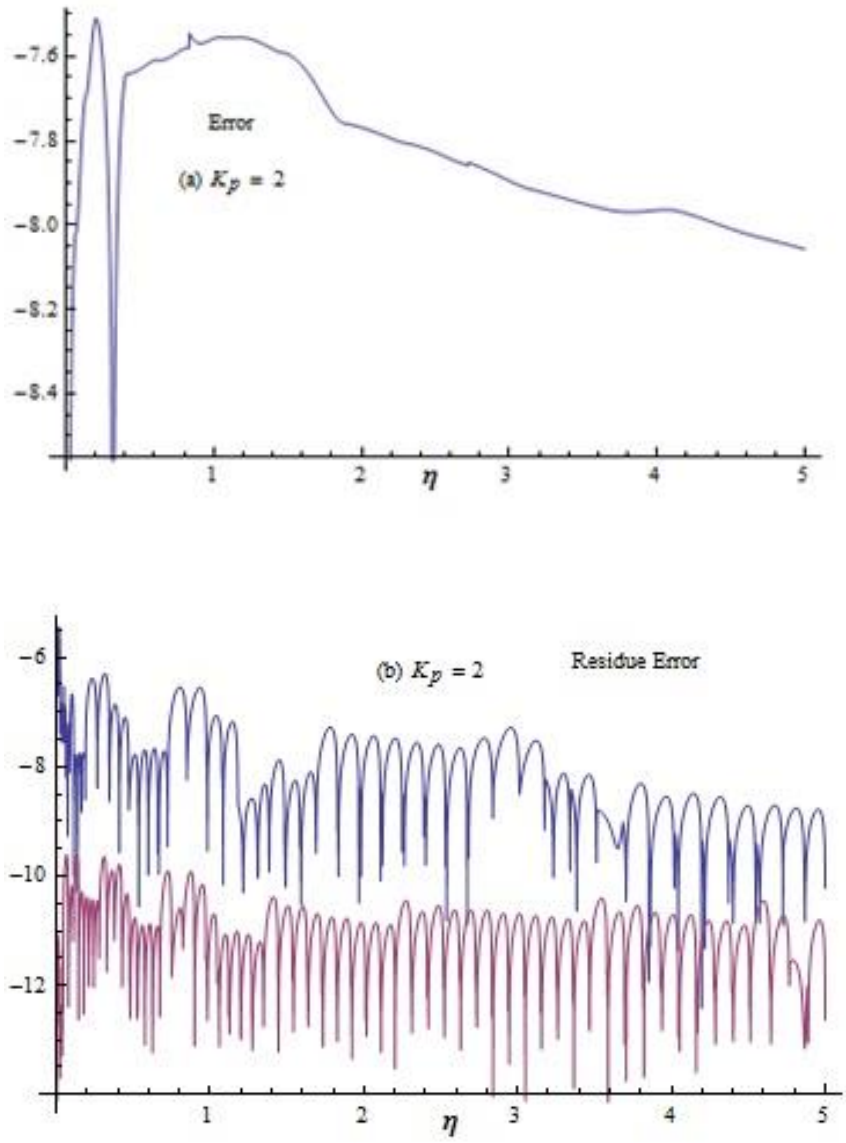

Figure 3(a-b). Error estimation for $K_p = 3$

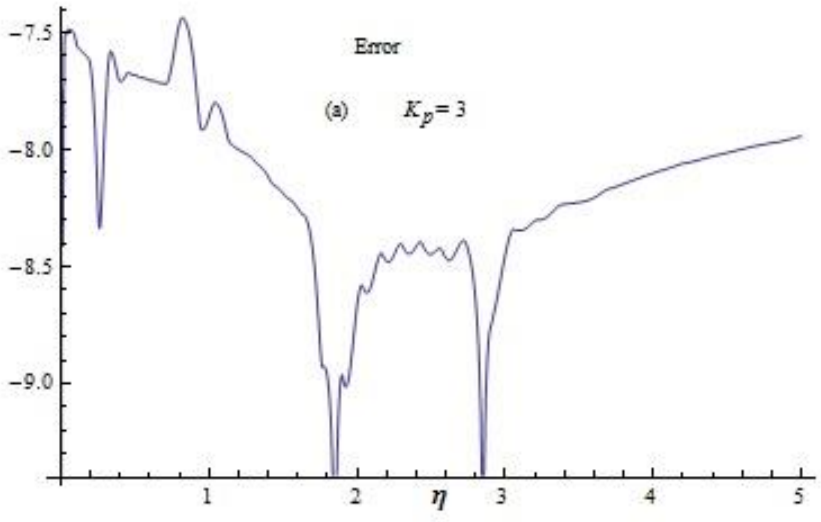

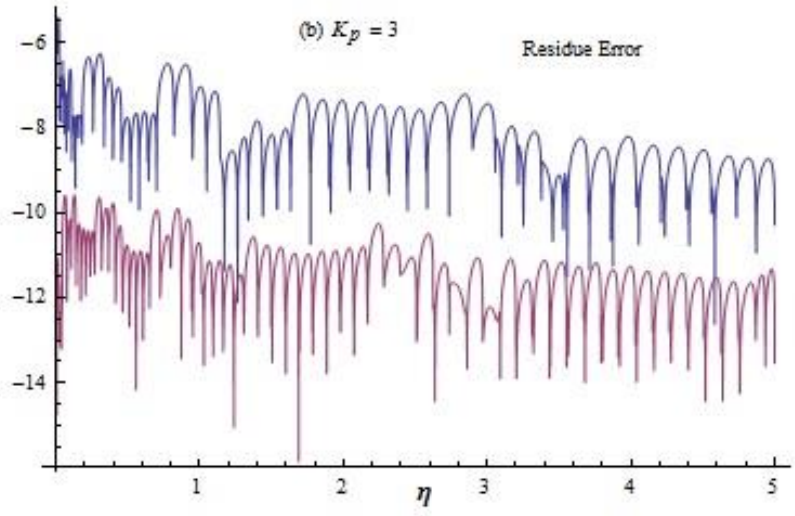

Figure 4(a-b). Error estimation for $K_p = 5$

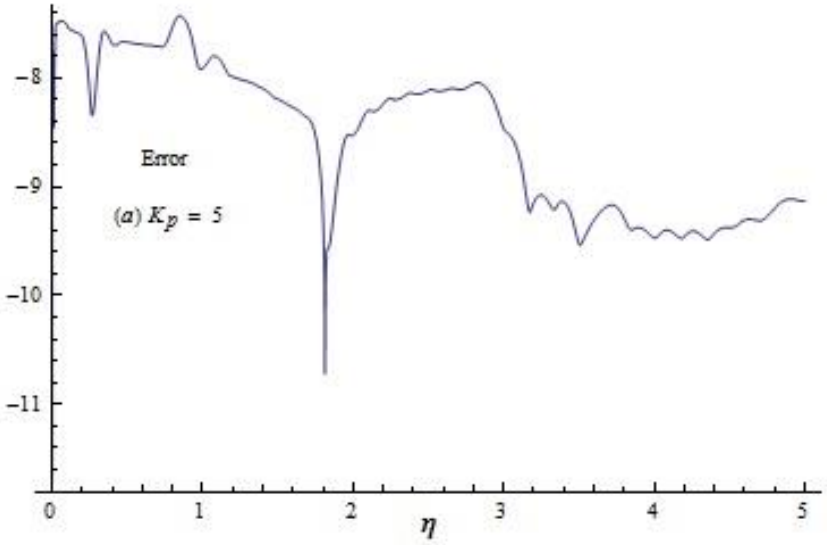

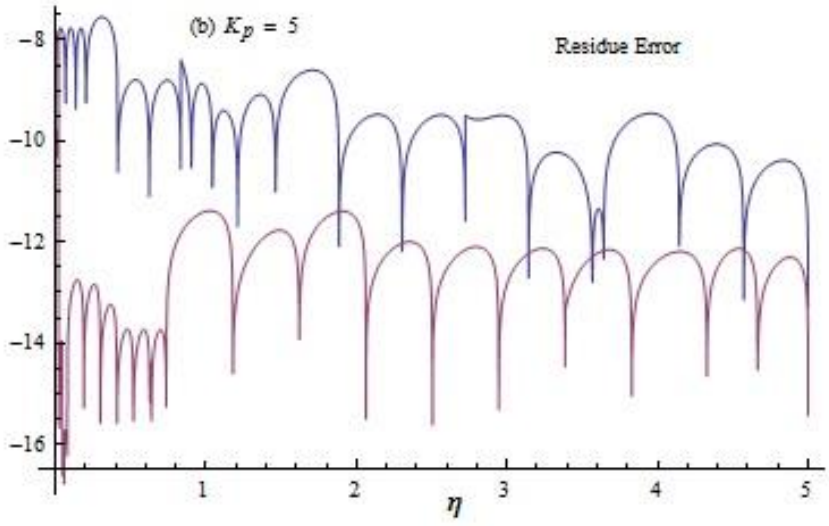

Figure 5(a-b). Error estimation for $\phi_2 = 0.2$

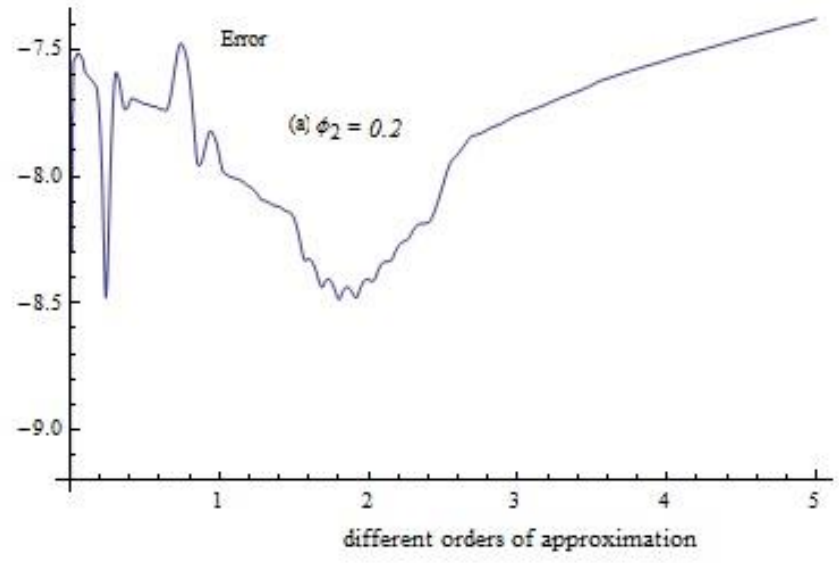

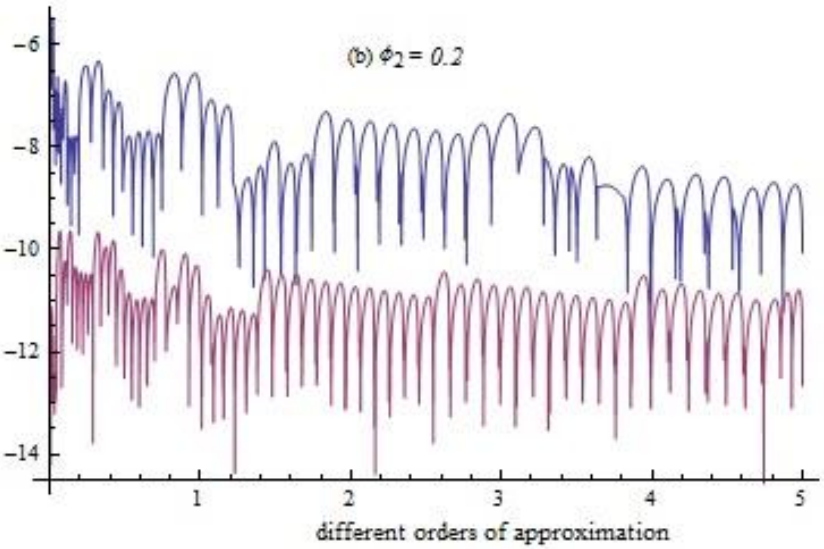

Figure 6(a-b). Error estimation for $\phi_2 = 0.0$

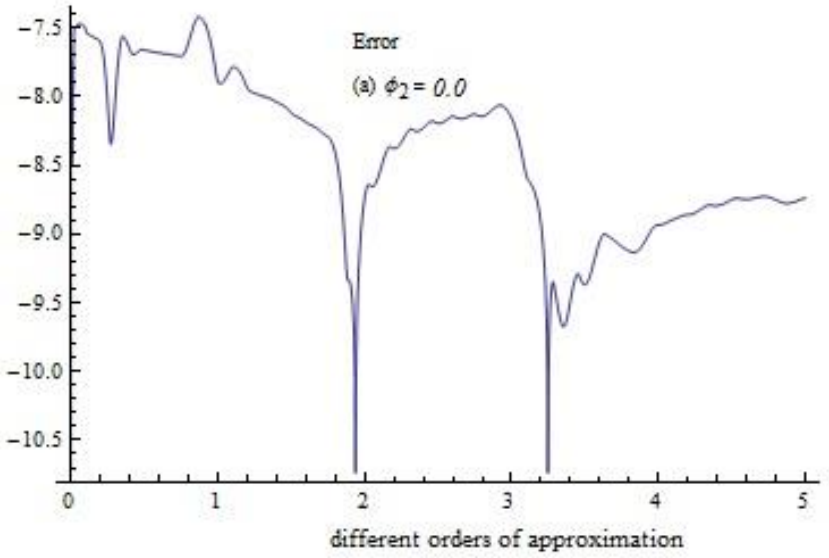

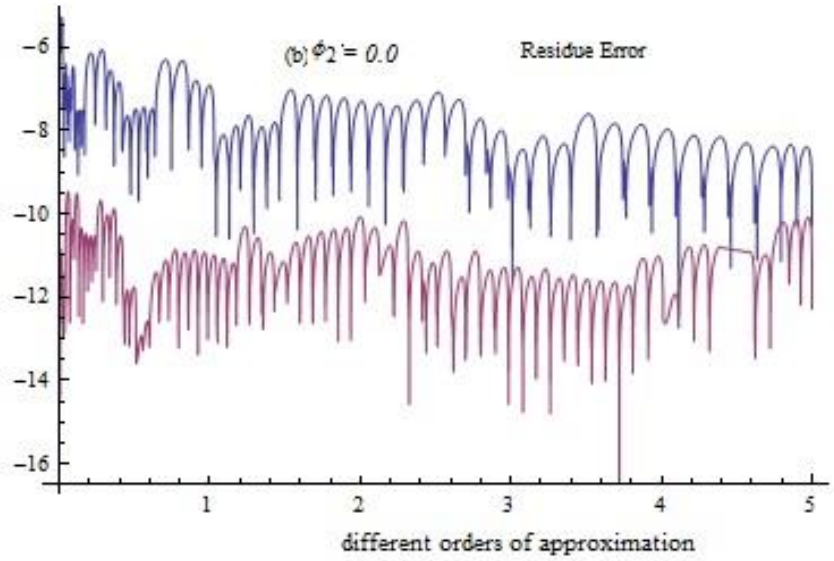

Figure 7(a-b). Error estimation for $\phi_2 = 0.1$

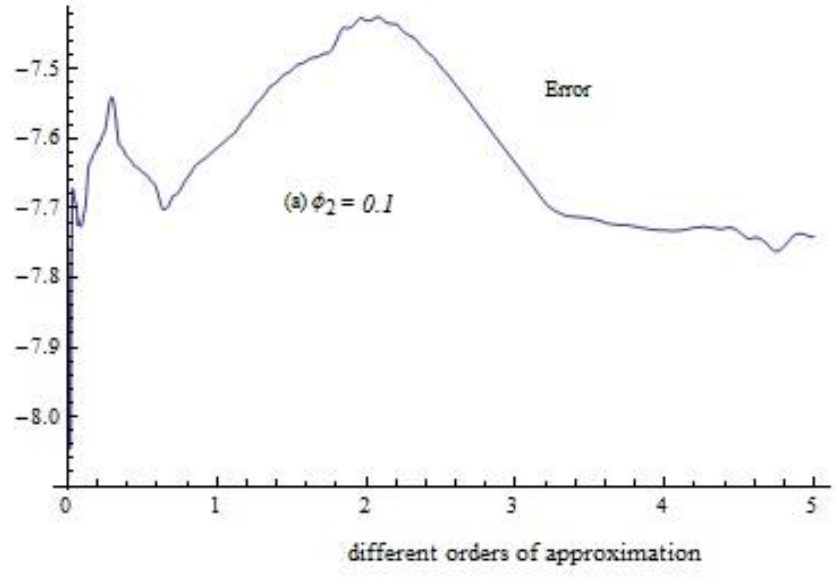

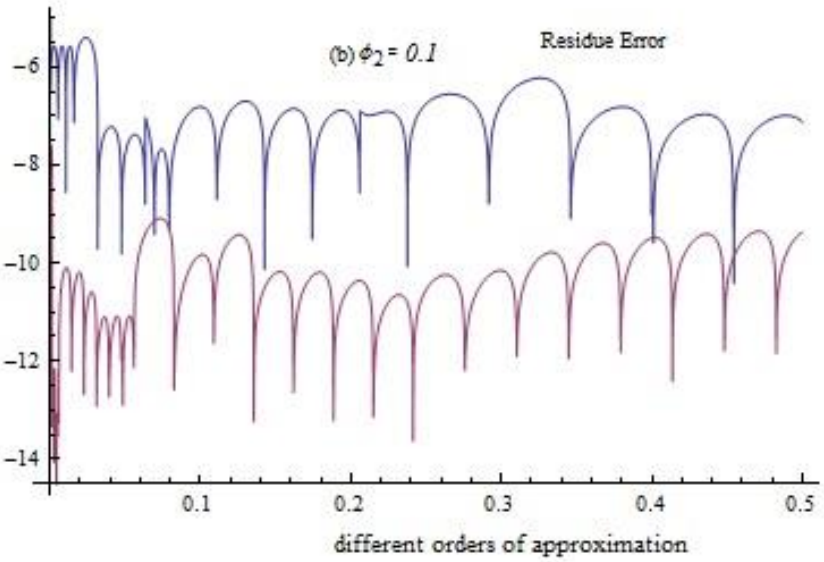

Figure 8(a-b). Error estimation for $\phi_2 = 1.0$.

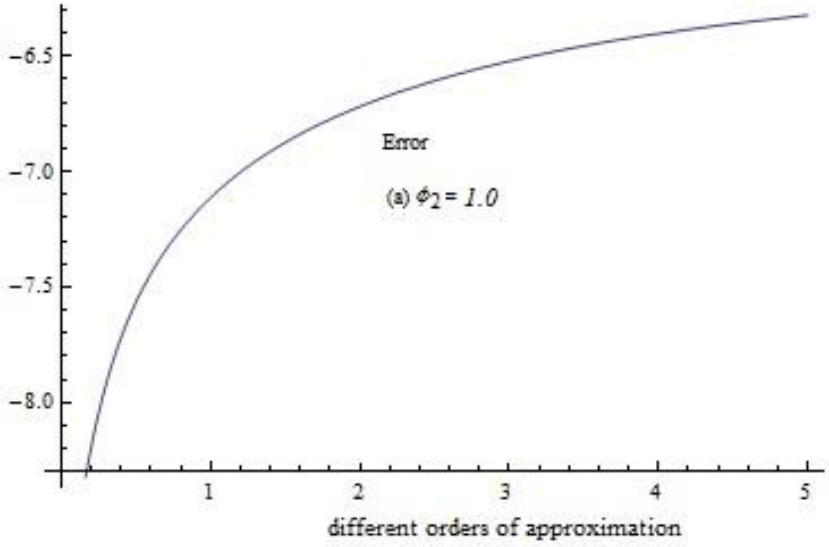

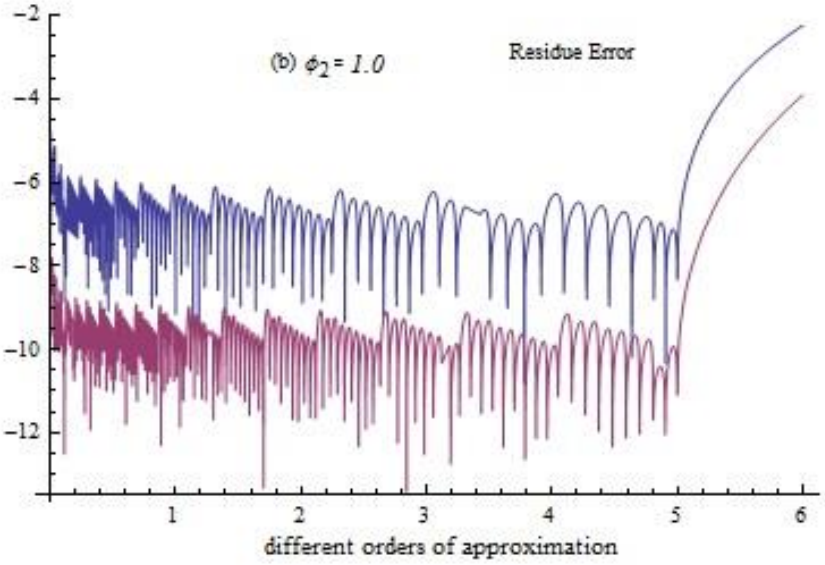

Figure 9. Motivation of K_p via DPV.

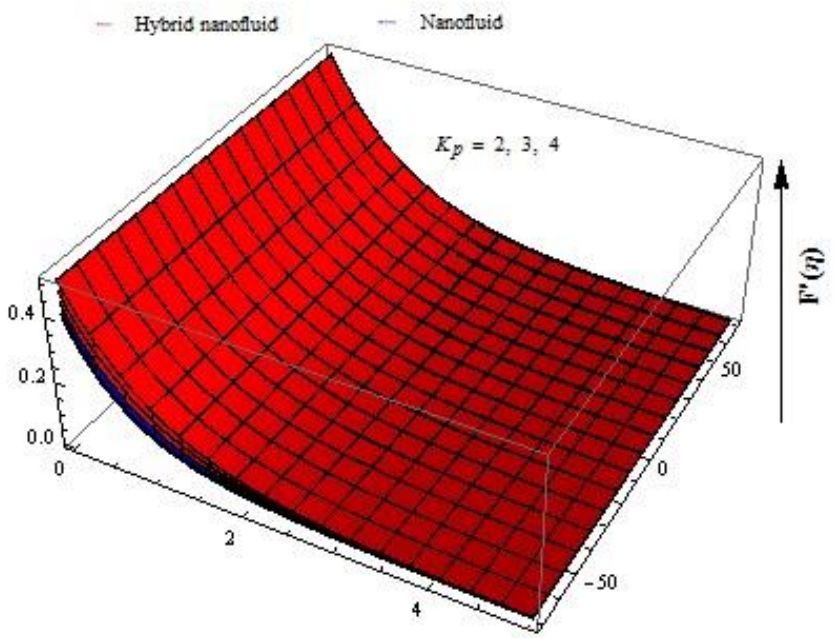

Figure 10. Motivation of K_p via DPT.

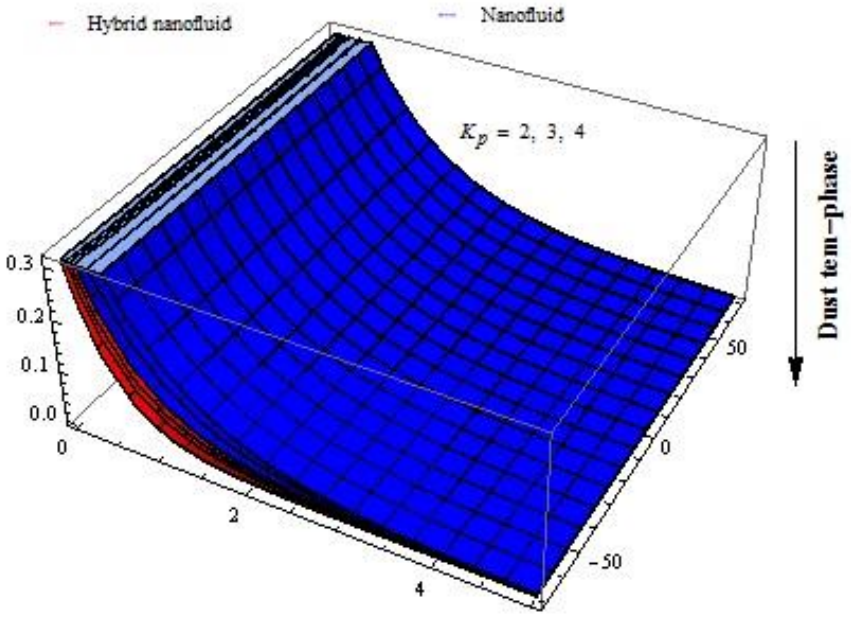

Figure11. Influence of ϕ_2 via velocity field.

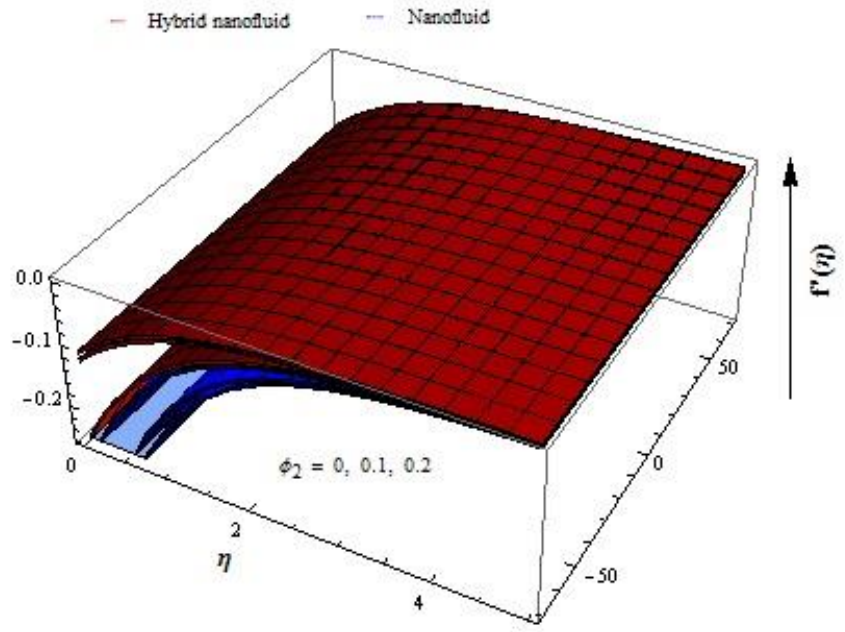

Figure12. Influence of ϕ_2 via DPV.

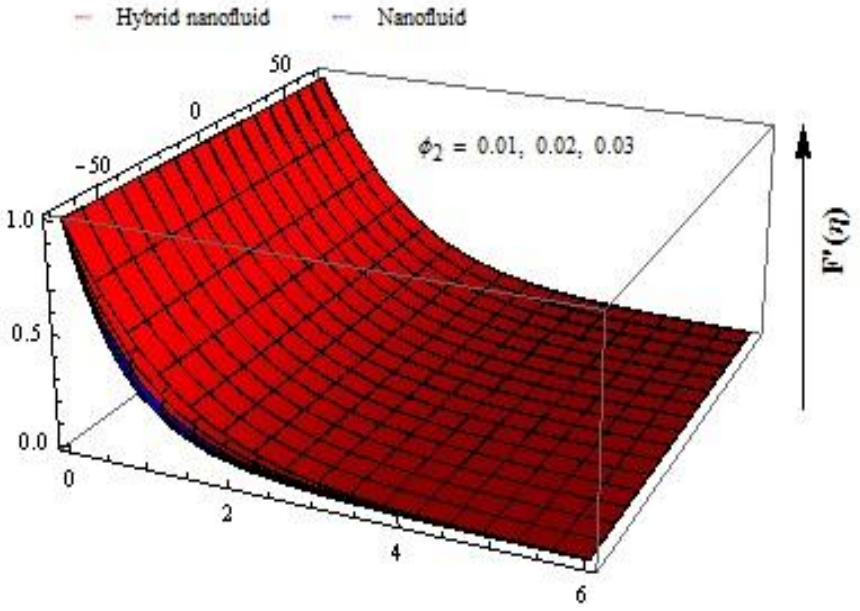

Figure13. Influence of ϕ_2 via with temperature field.

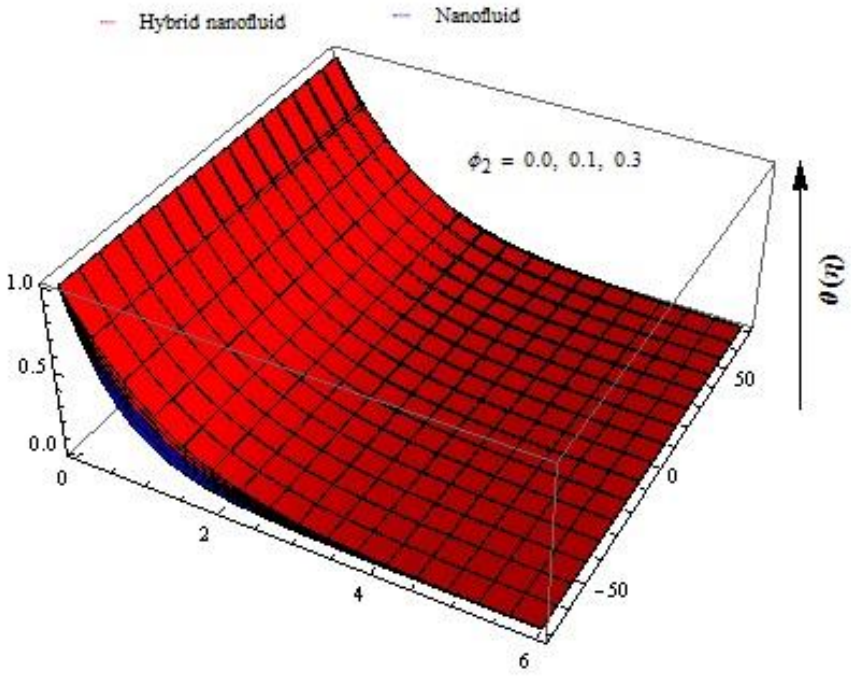

Figure14. Influence of ϕ_2 via DPT.

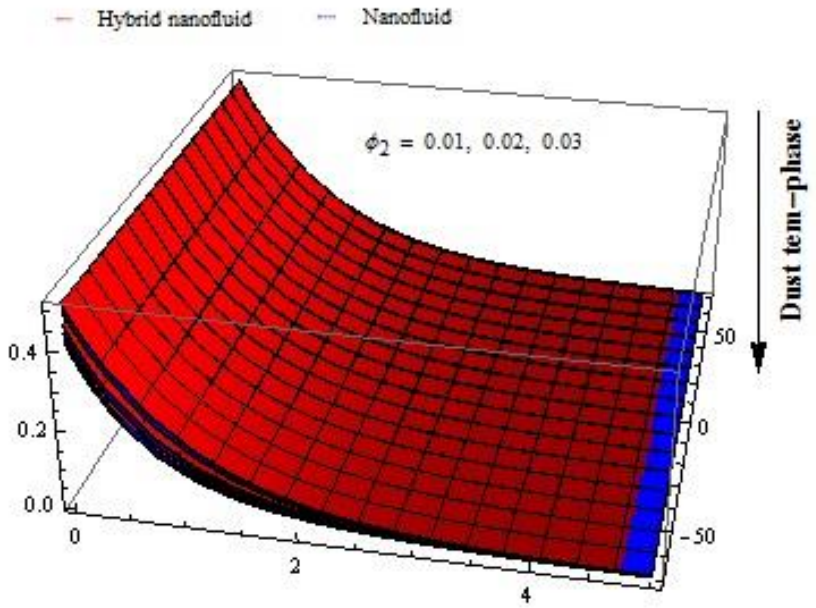

Figure15. Influence of L_0 via with velocity field.

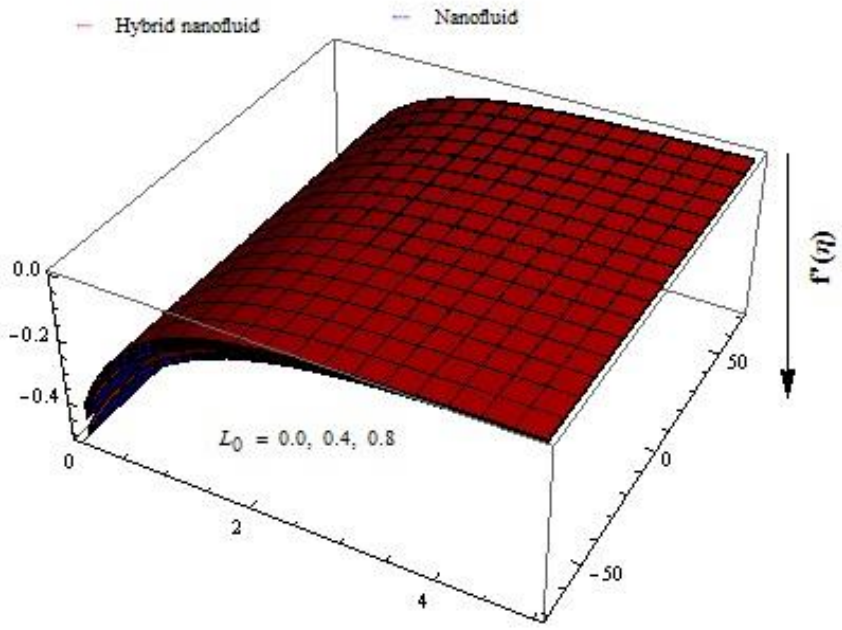

Figure16. Influence of L_1 via velocity field.

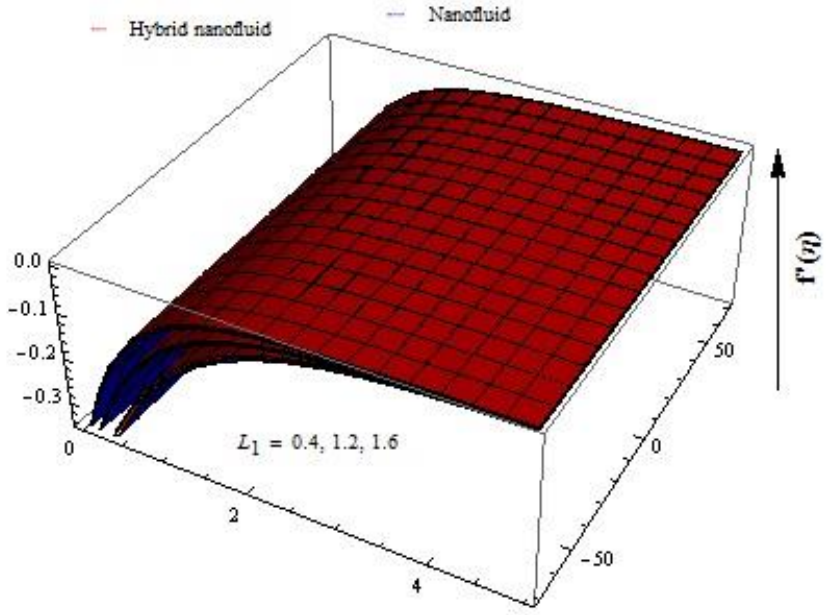

Figure17. Influence of M via velocity field.

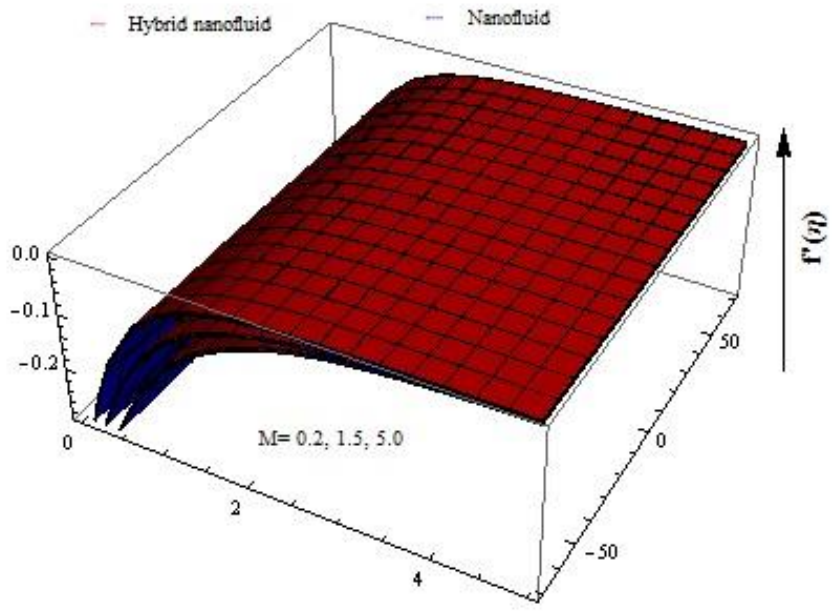

Figure18. Influence of B_v via DPV.

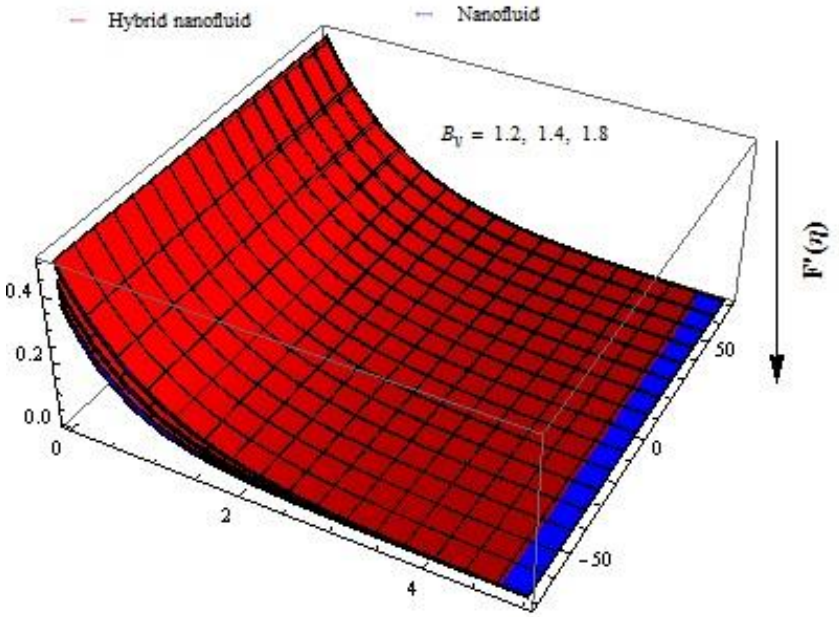

Figure19. Influence of M_d via DPV.

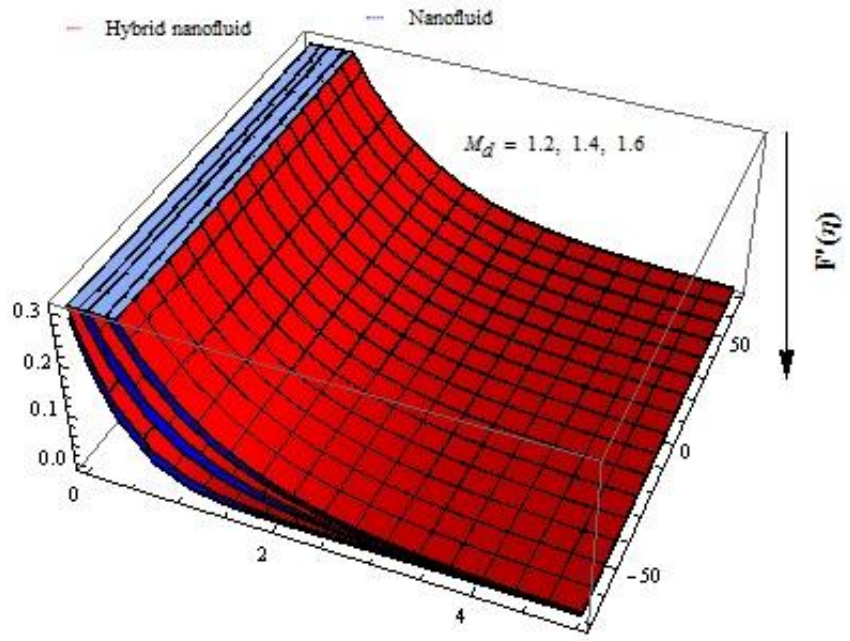

Figure20. Influence of ε_{Ther} via temperature field.

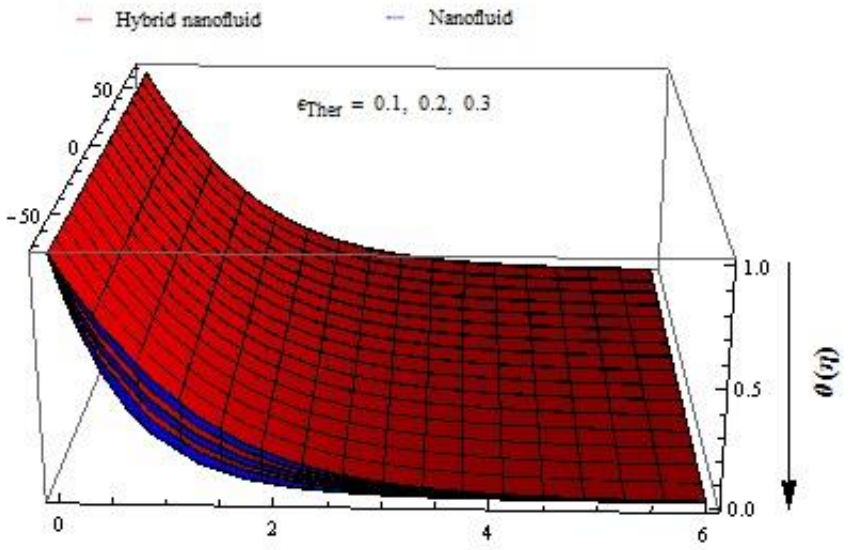

Figure21. Influence of γ via DPT.

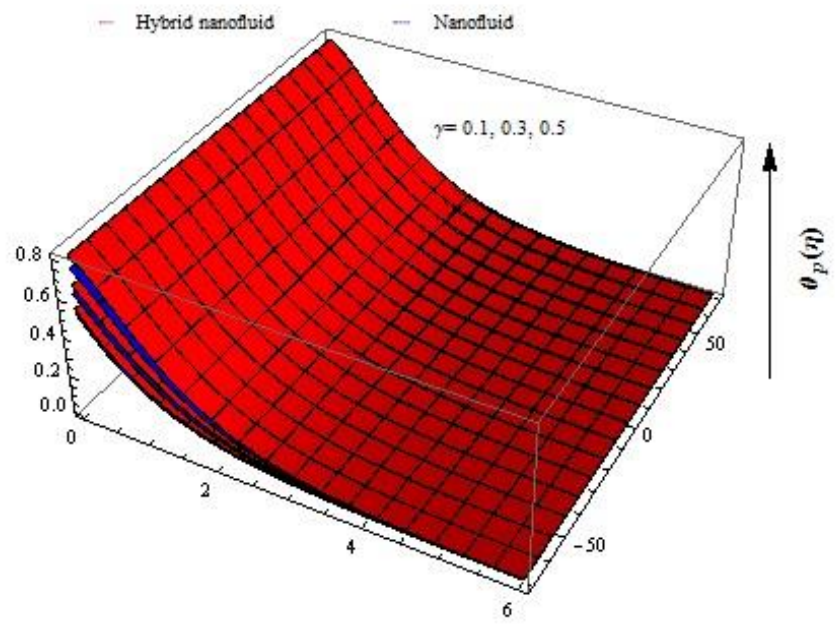

Figure22. Influence of *Ec* via temperature field.

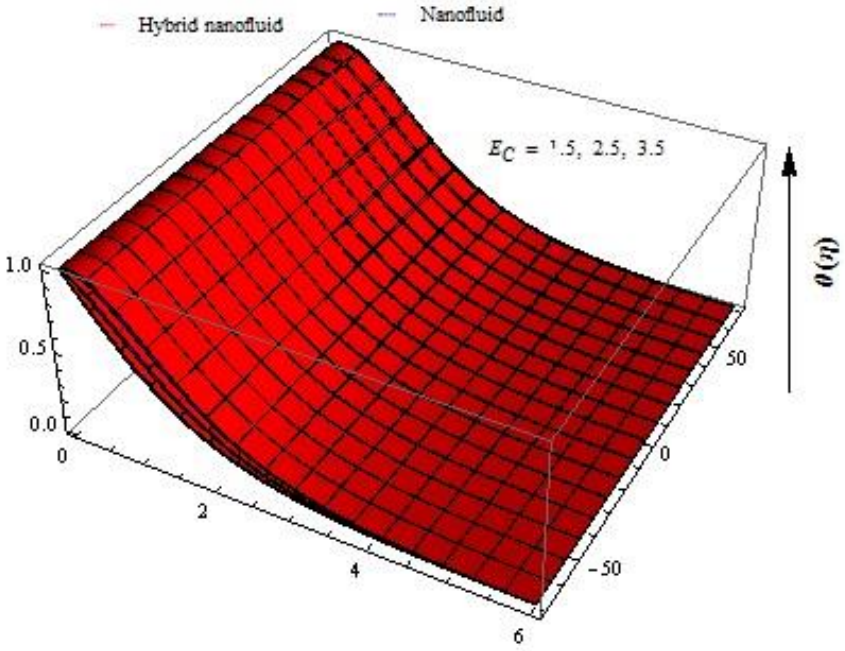

Table1. Thermo characteristics are given below [46, 47].

Base fluid/ Nanomaterial	C_p (J/kg K)	$\rho\left(Kg/m^3\right)z$	K(W/mK)
$C_2H_6O_2$	2430	1115	0.253
CuO	531.8	6320.0	76.5
Cu	385	8933	401

Table2: Assessment of present study to the previous $C_f\sqrt{\mathrm{Re}_s}$ by varying a_1 when $B_v = L_0 = 0 = L_1 = M = \phi_1 = \phi_2 = 0.$

K_p	Present work [47]	Published work
5	1.307800	1.307801
10	1.245511	1.245512
20	1.202502	1.202503
30	1.201700	1.201712
50	1.186401	1.186400
15	1.183311	1.183310
20	1.177013	1.177013

Table3: SF for different parameters fixing $\mathrm{Pr} = 5, B_v = 0.5, M_d = 10$ fixed.

Skin Friction						
ϕ_2	L_0	L_1	K_p	M	Nanofluid	Hybrid nanofluid
0.2	0.3	1.2	0.2	0.3	0.32633	0.47279
0.4					0.45774	0.50715
0.6					0.48215	0.54461
	0.2				0.51600	0.57181

	0.4				0.57313	0.63671
	0.6				0.64374	0.72053
		0.2			1.18620	1.38050
		0.3			0.68188	0.76388
		0.7			0.42330	0.47278
			2		0.68447	0.78638
			4		0.82715	0.80522
			5		0.82688	0.8818
				2	0.34740	0.38360
				3	0.31613	0.32224
				5	0.31527	0.31664